Visualization of Single Membrane Protein Structure in Stretched Lipid Bilayer Suspended over Nanowells

Youichi Shinozaki*, Koji Sumitomo, Kazuaki Furukawa, Hidetoshi Miyashita, Yukihiro Tamba, Nahoko Kasai, Hiroshi Nakashima, and Keiichi Torimitsu

NTT Basic Research Laboratories, NTT Corporation, 3-1 Morinosato Wakamiya, Atsugi, Kanagawa 243-0198, Japan

Received December 2, 2009; accepted December 29, 2009; published online January 29, 2010

In this study, we observed the topology of a single protein in a stretched lipid bilayer (membrane) suspended over a nanoscale well using a fast-scanning atomic force microscope (AFM). The membrane was located stably enough on the well to prevent the leakage of a liquid placed in the well, and it allowed us to observe membrane stretching using an AFM. We successfully observed the gradual stretching of the suspended membrane. We also observed single bacteriorhodopsin proteins in the stretched membrane, and found that they maintained their trimeric structure, but that the distances between the trimers increased.

DOI: 10.1143/APEX.3.027002

Nanotechnology offers the prospect of realizing novel materials and devices on a nanometer scale. Recent advances in nanotechnology have provided novel techniques that give us new insights into the biological sciences. In this field, nanofabricated materials are used to detect, diagnose, and regulate biological molecules and cells: quantum nanoparticles are employed to detect biomolecules or cells;[1] quantum particles are used for diagnosis and are a potential treatment for cancer;[2] biomaterials are used for tissue engineering;[3] nanopillars are employed for the manipulation and separation of DNA;[4] microchannels are used for cell separation;[5] single-wall carbon nanotubes or nanohorns are used as drug delivery systems.[6,7]

Our group also uses micro- or nanofabricated structures to study biological issues. We fabricated microchannels[8,9] and microchannels with a sub-100-nm gap (nano-gap)[10] to analyze the self-spreading behavior of a supported lipid bilayer (membrane) on a solid substrate. In another study, we used nanotrenches to estimate the elastic modulus of a purple membrane (PM).[11] The PM was obtained from *Halobacterium salinarium* and composed of 25% lipids and 75% bacteriorhodopsins (BRs).[12] When the PM was suspended over a sub-micron (i.e., 500 nm diameter) well, we could not observe BRs on a molecular scale, because the membrane was unstable on a well of this width. On the other hand, a suspended PM supported by carbon nanotubes (CNTs) allowed us to observe molecular scale BRs.[13] The unsupported PM was disturbed by the tip of the atomic force microscope (AFM) during scanning, and it was difficult to obtain molecular images. A smaller well diameter and fast scanning minimized the effect of this disturbance. In the present study, we set the well diameter at 100 nm and employed a fast-scanning AFM to observe the molecular-scale topology of samples (i.e., lipid membrane or PM) suspended over a well without CNT support. The AFM observation of single proteins in a membrane suspended over holes has already been achieved by the other group.[14] They reported the molecular structures of a suspended S-layer membrane of *Corynebacterium glutamicum* over a hole. We observed a PM and employed a fast-scanning AFM because the BRs in a PM are the best-studied seven-helix membrane proteins. Various techniques including atomic force microscopy, and fast scanning have been employed for the molecular-scale imaging of these proteins. BRs are structurally similar to important cellular signaling proteins namely G-protein-coupled membrane receptors (GPCRs),[15] the largest family of seven-helix membrane proteins. Although some GPCR structures have already been clarified, BR data obtained with an AFM are still useful for studying the relationships between the structure and function of seven-helix membrane proteins. Structural changes are important with respect to GPCR activity: when GPCRs are activated, their structures change within a subunit, and some GPCRs exhibit changes in stoichiometry (i.e., changes between monomer and oligomer).[16] Because an AFM can detect monomeric (or oligomer subunit) seven-helix membrane proteins, at least the latter reaction can be visualized by AFM. In addition to visualizing topology, an AFM can be used to stretch a membrane suspended over a well. In fact, an AFM is used as a microindentor to investigate the mechanism of strain-induced responses in cells.[17] The mechanical stimulation of cells induces one of the most important biological signals that underlies many essential functions including blood pressure regulation, vascular responses, bone remodeling, muscle maintenance, and the senses of touch and hearing.[18–20] Mechanical stimulation activates a certain group of proteins that are sensitive to mechanical stress (i.e., mechanosensitive proteins). These proteins include GPCRs.[21] Although some mechanical proteins have been identified, their details, and other candidates for mechanosensitive proteins, remain to be clarified. In this study, we describe the molecular-scale topology of proteins in a stretched membrane using a fast-scanning AFM.

We first fabricated wells on a silicon substrate as reported previously.[11] The membrane was prepared on the substrate by vesicle fusion. The vesicle was formed by sonicating a mixture of lipids [a 1 : 4 ratio of *N*-(fluorescein-5-thiocarbamoyl)-1,2-dihexadecanoyl-*sn*-glycero-3-phosphoethanolamine (fluorescein-DHPE):L-α-phosphatidylcholine (L-α-PC), 500 μg/ml] and Tris buffer (10 mM Tris–HCl, pH 8.0). After a few hours of incubation at room temperature (RT), we obtained a mixture of small (SUVs) and large unilamellar vesicles (LUVs) [100–1000 nm in diameter, estimated by dynamic light scattering (data not shown)]. The diameter of the well was set at 100 nm (with a 500 nm pitch), and we made the surface of the substrate hydrophilic as previously reported.[11] Then we checked

*E-mail address: shinozak@will.brl.ntt.co.jp

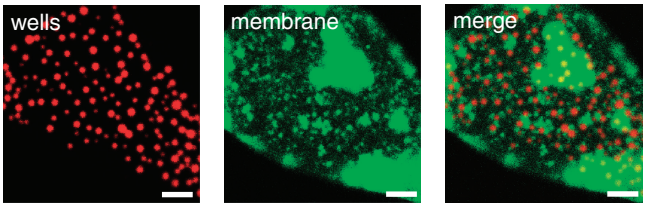

Fig. 1. Wells containing ATP-Alexa 594 (a) and wells covered with green fluorescent-labeled membrane (b). (c) The membrane-covered area corresponds well with the area exhibiting red spots.

whether the well was filled with liquid after covering it with the membrane. The lipid vesicles were mixed with ATP-Alexa 594 (1 mM), placed on the substrate, $CaCl_2$ (2 mM) was added, and the result was incubated for 1 h at RT. The buffer outside the well was renewed 10 times, and the sample was observed with a confocal laser scanning microscope BX51-FV300 (Olympus) under a ×10 objective lens. We used laser light sources emitting at 488 and 543 nm for excitation, a 505–525 nm filter (for fluorescein) and 610 nm high-pass filters (for Alexa 594). Red fluorescent spots (from Alexa 594) were observed only on part of the substrate [Fig. 1(a)]. The membrane-covered area was detected by green fluorescent signals (from fluorescein) [Fig. 1(b)]. The ununiformity of green fluorescent intensity might be caused by either the difference of the density of a small lipid patch or by a phase separation. The membrane area corresponded well to the region exhibiting red spots [Fig. 1(c)], indicating that the wells were successfully sealed. The red spots were larger than the actual well diameter owing to the limited spatial resolution of the fluorescent microscope. Also, these spots were not in ordered alignment even though the wells were arranged in order. During vesicle fusion, the dye-containing liquid inserted in some of the wells appeared to be replaced with liquid from the vesicle. The red spots were observed after a further 1 hr of incubation. This suggests that sealing the well with the membrane is sufficient to prevent dye leakage.

Next we observed a membrane suspended over a well using an NVB500 fast-scanning AFM with a BL-AC7EGS-A2 cantilever that had a spring constant of 0.1–0.3 N/m (Olympus, Tokyo, Japan). For the AFM observation, we used a lipid mixture consisting of a 75 : 23 : 2 ratio of 1,2-dipalmitoyl-*sn*-glycero-3-phosphocholine (DPPC), 1,2-dilauroyl-*sn*-glycero-3-phosphate (DLPA), and 1,2-dipalmitoyl-*sn*-glycero-3-phosphothioethanol (DPPTE) (200 μg/ml). The lipid vesicles were placed on the substrate, and then $CaCl_2$ (2 mM) was added and incubated for 30 min at 55 °C. Figure 2(a) shows an AFM image of the membrane-coated well. The AFM images are presented as gray-scale height images. The bare well was deeper than the surface of the substrate [Fig. 2(a), asterisk], but the well covered by the membrane had a similar height to the membrane-covered substrate [Fig. 2(a), arrow], indicating that the membrane on the well was flat. We gradually stretched the suspended membrane by increasing the imaging force [Fig. 2(b), 0–100 s]. When the stretching was stopped, the membrane became flat again following the stress relaxation [Fig. 2(b), 120 s], indicating the membrane flexibility. The membrane was then stretched again. When the membrane was stretched to a depth of over 20 nm [Fig. 2(c), 36 s], it punctured [Fig. 2(c), 37 s], and the membrane was stripped from the substrate [Fig. 2(c), 50 s]. This system allows us to perform simultaneous experiments involving membrane stretching and the imaging of a suspended membrane at high spatial (i.e., nanometer level) and temporal (i.e., down to 100 ms/frame) resolution. In this study, we obtained data at 500 ms/frame.

We then observed a PM on mica or over a well. The PM was suspended in Tris buffer (10 mM Tris–HCl, pH 8.0, at 5 μg/ml), placed on mica, and incubated for 30 min at room temperature (RT). Unadsorbed PMs were removed by washing 10 times with Tris buffer. The mica-supported PM was about 5 nm thick [Fig. 3(a), center] and had the trimeric and three-fold symmetry structure of BRs [Fig. 3(a), right], which agrees well with previous reports.[22,23] When the PM was suspended over the well [Fig. 3(b), left, rectangle], a cross-section of the covered well was shallower than that of an uncovered one [Fig. 3(b), center, arrowhead]. An enlarged image of the rectangle [Fig. 3(b), left] (i.e., the suspended PM) showed that the ordered structure was disrupted but a trimer-like structure was maintained even in a stretched condition [Fig. 3(b), right]. The suspended purple membrane was stretched by 40% [Fig. 4(a)]. Meanwhile, the average distance between BR timers on mica was 6.6 ± 0.1 nm ($n = 30$), and that between trimers over the well was 9.6 ±

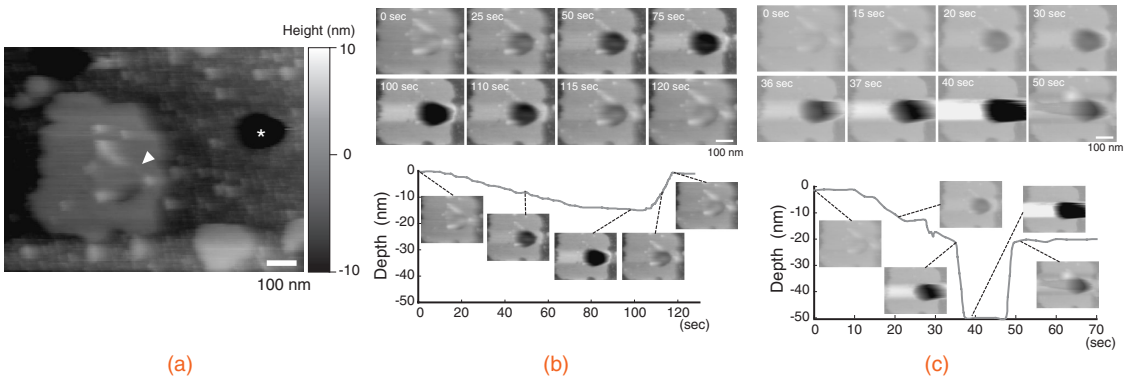

Fig. 2. (a) Uncovered wells (∗) and wells covered with a membrane (arrow). (b) When the degree of membrane stretching was small (<20 nm in depth), the membrane recovered its flatness. (c) The membrane was disrupted with excess stretching (at 37 s). The lower panels show the depth of the membrane surface at each time point.

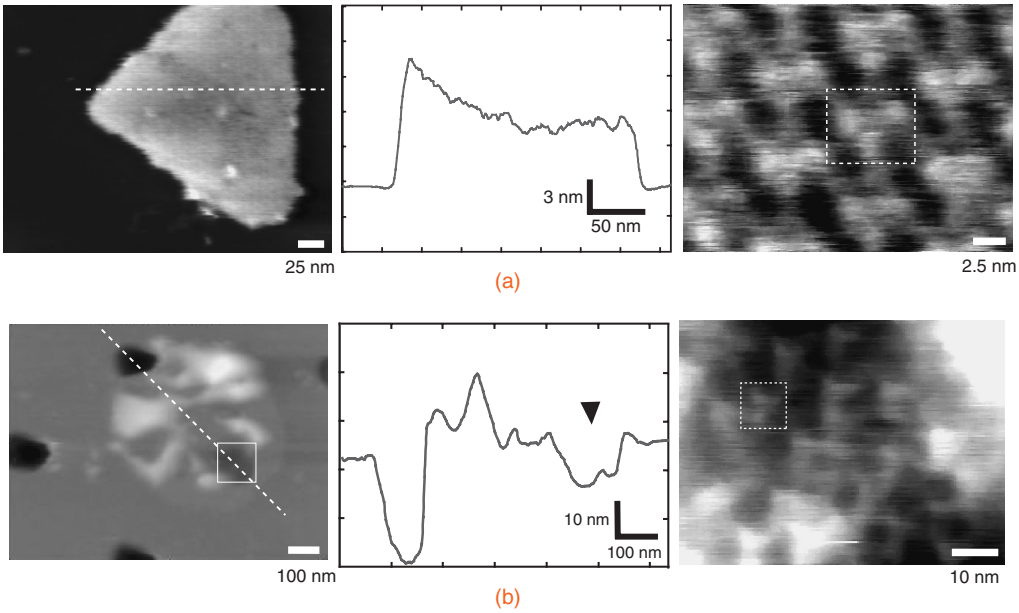

Fig. 3. (a) A purple membrane on mica exhibited a patch structure (left) and BRs were highly ordered with a trimeric structure (right, rectangle). A cross-section of the purple membrane was 5 nm thick (center). (b) BRs over a well. A cross-section of BRs over a well (the broken line, left panel) exhibits sealing by a membrane (arrow, center panel). (c) BRs in a stretched membrane maintain a trimeric structure but disrupted the ordered structure.

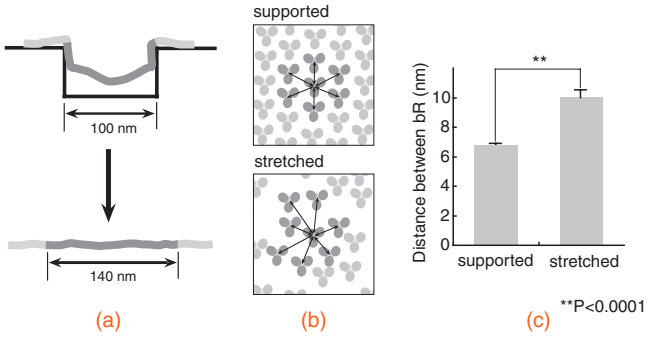

Fig. 4. (a) The stretched membrane suspended over the well is about 140 nm long, or 40% longer than the hole diameter. (b) Schematics illustrating criteria for measuring distances between trimers. (c) The distances between adjacent BR trimers were 6.6 ± 0.1 nm ($n = 30$, on mica), and 9.6 ± 0.5 nm ($n = 42$, on a well), respectively ($^{**}P < 0.0001$, the mean ± SEM, Student's t-test).

0.5 nm ($n = 42$) [Fig. 4(b)]. The distance between trimers on the well was about 40% greater than that on mica [Fig. 4(c), $^{**}P < 0.0001$]. The average results were expressed as mean ± standard error mean (SEM). Data were analyzed with the Student's t-test to determine the differences between groups. Significance was accepted when $p < 0.05$.

To our knowledge, our data is the first demonstration of the molecular imaging of BRs in a suspended/stretched PM. The mechanosensitivity of proteins is an essential issue, however, the mechanisms and other mechanosensitive proteins remain to be clarified owing to the lack of an experimental system that detects the molecular structure of proteins under a stretched condition. As our system enables us to observe the molecular structure of proteins under a stretched condition, it will help us to analyze membrane stretch-induced structural changes in proteins.

Acknowledgment This study was supported in part by a Grant-in-Aid for Scientific Research B20360014 from the Japan Society for the Promotion of Science (JSPS).

1) C.-Y. Zhang, H.-C. Yeh, M. T. Kuroki, and T.-H. Wang: Nat. Mater. **4** (2005) 435.
2) R. Bakalova, H. Ohba, Z. Zhelev, T. Nagase, R. Jose, M. Ishikawa, and Y. Baba: Nano Lett. **4** (2004) 1567.
3) K. Ohashi, T. Yokoyama, M. Yamato, H. Kuge, H. Kanehiro, M. Tsutsumi, T. Amanuma, H. Iwata, J. Yang, T. Okano, and Y. Nakajima: Nat. Med. **13** (2007) 880.
4) M. Tabuchi, M. Ueda, N. Kaji, Y. Yamasaki, Y. Nagasaki, K. Yoshikawa, K. Kataoka, and Y. Baba: Nat. Biotechnol. **22** (2004) 337.
5) T. Tachi, N. Kaji, M. Tokeshi, and Y. Baba: Anal. Chem. **81** (2009) 3194.
6) J. Chen, S. Chen, X. Zhao, L. V. Kuznetsova, S. S. Wong, and I. Ojima: J. Am. Chem. Soc. **130** (2008) 16778.
7) M. Zhang, T. Murakami, K. Ajima, K. Tsuchida, A. S. D. Sandanayaka, O. Ito, S. Iijima, and M. Yudasaka: Proc. Natl. Acad. Sci. U.S.A. **105** (2008) 14773.
8) K. Furukawa, H. Nakashima, Y. Kashimura, and K. Torimitsu: Langmuir **24** (2008) 921.
9) K. Furukawa, H. Nakashima, Y. Kashimura, and K. Torimitsu: Lab Chip **6** (2006) 1001.
10) Y. Kashimura, J. Durao, K. Furukawa, and K. Torimitsu: Jpn. J. Appl. Phys. **47** (2008) 3248.
11) A. M. Siitonen, K. Sumitomo, C. S. Ramanjuan, Y. Shinozaki, N. Kasai, K. Furukawa, J. F. Ryan, and K. Torimitsu: Appl. Surf. Sci. **254** (2008) 7877.
12) I. Szundi and W. Stoeckenius: Proc. Natl. Acad. Sci. U.S.A. **84** (1987) 3681.
13) K. Sumitomo, Y. Shinozaki, D. Takagi, H. Nakashima, Y. Kobayashi, and K. Torimitsu: Jpn. J. Appl. Phys. **48** (2009) 08JB18.
14) R. P. Gonçalves, G. Agnus, P. Sens, C. Houssin, B. Bartenlian, and S. Scheuring: Nat. Methods **3** (2006) 1007.
15) T. Hirai, S. Subramaniam, and J. K. Lanyi: Curr. Opin. Struct. Biol. **19** (2009) 433.
16) V. V. Gurevich and E. V. Gurevich: Trends Neurosci. **31** (2008) 74.
17) G. T. Charras and M. A. Horton: Biophys J. **82** (2002) 2970.
18) G. G. Ernstrom and M. Chalfie: Annu. Rev. Genet. **36** (2002) 411.
19) P. F. Davies: Physiol. Rev. **75** (1995) 519.
20) S. Lehoux and A. Tedgui: J. Biomech. **36** (2003) 631.
21) Y. Zou, H. Akazawa, Y. Qin, M. Sano, H. Takano, T. Minamino, N. Makita, K. Iwanaga, W. Zhu, S. Kudoh, H. Toko, K. Tamura, M. Kihara, T. Nagai, A. Fukamizu, S. Uemura, T. Iiri, T. Fujita, and I. Komuro: Nat. Cell. Biol. **6** (2004) 499.
22) D. J. Müller, H.-J. Sass, S. A. Müller, G. Büldt, and A. Engel: J. Mol. Biol. **285** (1999) 1903.
23) Y. Jin, N. Friedman, M. Sheves, T. He, and D. Cahen: Proc. Natl. Acad. Sci. U.S.A. **103** (2006) 8601.